Genomics 113 (2021) 3919–3934

Contents lists available at ScienceDirect

Genomics

journal homepage: www.elsevier.com/locate/ygeno

Transcriptional characterization of subcutaneous adipose tissue in obesity affected women highlights metabolic dysfunction and implications for lncRNAs

Federica Rey [a,b,1], Letizia Messa [c,1], Cecilia Pandini [d], Bianca Barzaghini [c], Giancarlo Micheletto [e], Manuela Teresa Raimondi [c], Simona Bertoli [f,g], Cristina Cereda [d,2], Gian Vincenzo Zuccotti [a,b,h], Raffaella Cancello [f,3], Stephana Carelli [a,b,3,*]

[a] Department of Biomedical and Clinical Sciences "L. Sacco", University of Milan, Via Grassi 74, 20157 Milan, Italy
[b] Pediatric Clinical Research Centre Fondazione "Romeo ed Enrica Invernizzi", University of Milano, Milano, Italy
[c] Department of Chemistry, Materials and Chemical Engineering "Giulio Natta", Politecnico di Milano, Milano, Italy
[d] Genomic and post-Genomic Centre, IRCCS Mondino Foundation, 27100 Pavia, Italy
[e] Department of Pathophysiology and Transplantation, INCO, Department of General Surgery, Istituto Clinico Sant'Ambrogio, University of Milan, Milan, Italy
[f] Obesity Unit, Laboratory of Nutrition and Obesity Research, Department of Endocrine and Metabolic Diseases, IRCCS Istituto Auxologico Italiano, Milan, Italy
[g] International Center for the Assessment of Nutritional Status (ICANS), Department of Food, Environmental and Nutritional Sciences (DeFENS), University of Milan, Milan, Italy
[h] Department of Pediatrics, Children's Hospital "V. Buzzi", Milan, Italy

ARTICLE INFO

Keywords:
Obesity
Transcriptome
RNA-seq
lncRNAs
Gene expression
Metabolic diseases

ABSTRACT

Obesity is a complex disease with multifactorial causes, and its prevalence is becoming a serious health crisis. For this reason, there is a crucial need to identify novel targets and players. With this aim in mind, we analyzed via RNA-sequencing the subcutaneous adipose tissue of normal weight and obesity-affected women, highlighting the differential expression in the two tissues. We specifically focused on long non-coding RNAs, as 6 of these emerged as dysregulated in the diseased-tissue (COL4A2-AS2, RPS21-AS, PELATON, ITGB2-AS1, ACER2-AS and CTEPHA1). For each of them, we performed both a thorough in silico dissection and in vitro validation, to predict their function during adipogenesis. We report the lncRNAs expression during adipose derived stem cells differentiation to adipocytes as model of adipogenesis and their potential modulation by adipogenesis-related transcription factors (C/EBPs and PPARγ). Moreover, inhibiting CTEPHA1 expression we investigated its impact on adipogenesis-related transcription factors, showing its significative dysregulation of C/EBPα expression. Lastly, we dissected the subcellular localization, pathway involvement and disease-correlation for coding differentially expressed genes. Together, these findings highlight a transcriptional deregulation at the basis of obesity, impacted by both coding and long non-coding RNAs.

1. Introduction

Obesity is defined as abnormal or excessive fat accumulation, presenting a risk to health [1]. The most recent update of the World Health Organization (WHO) reports how the worldwide prevalence of obesity nearly tripled between 1975 and 2016, with over 650 million adults being clinically defined as obese [1]. The most significant implication is the increased risk of co-morbidities development, such as type 2 diabetes (T2D), hypertension, dyslipidemia, coronary artery disease, stroke, osteoarthritis and even certain forms of cancer increasing mortality and direct and indirect socioeconomic costs [1–4]. Canonical approaches to counteract obesity involve decreasing energy intake by choosing a

* Corresponding author at: Pediatric Clinical Research Center Fondazione "Romeo ed Enrica Invernizzi", University of Milano, Milano, Italy.
E-mail address: stephana.carelli@unimi.it (S. Carelli).
[1] These authors contributed equally to the work.
[2] Present address: Cristina Cereda, Department of Women, Mothers and Neonatal Care, Children's Hospital "V. Buzzi", Milan, Italy mail: cristina.cereda@asst-fbf-sacco.it
[3] These authors contributed equally to the work.

https://doi.org/10.1016/j.ygeno.2021.09.014
Received 18 May 2021; Received in revised form 3 September 2021; Accepted 17 September 2021
Available online 21 September 2021

suitable diet and increasing the energy expenditure with exercise, but these two approaches alone are not always sufficient [5]. There is thus a need to identify and characterize novel implicated targets, in order to identify new regulators in disease pathogenesis along with novel potential therapeutic targets. The identification of genes implicated in obesity development has been possible thanks to Genome Wide Association Studies, which have allowed the identification of mutations and polymorphisms which can be associated to BMI increase, waist circumference, and waist-to-hip ratio [6]. To date, more than 97 loci related to complex obesity that account for approximately 2.7% of BMI, waist circumference, and waist-to-hip ratio variations have been identified [6]. Even so, it is not possible to claim that obesity can be caused either by the genes or the environment, but it is rather possible to state that behavior and genes are different levels of the same causal framework [7–9]. In this context, epigenetic aspects need to be considered as they are crucial regulators in the translation of environment stimuli on gene expression regulation [7–9].

In recent years, the role of the transcriptome is taking on prominence and its relevance in the regulation of biologic processes is now reconsidered since up to 90% of the genome is transcribed and not translated into a protein [10]. Amongst the epigenetic modulators there are also small non-coding RNAs, which include micro RNAs (miRNA), and long non-coding RNAs (lncRNAs), subdivided according to their dimension [10]. These transcripts are relevant also in the field of adipogenesis, fat mass expansion and obesity. High throughput screening have allowed for the identification of novel targets, at both coding and non-coding levels. Proteomics studies have been performed highlighting deregulated proteins in adipose tissue of obesity-affected patients [11]. Moreover, miRNAs have been found to play regulatory roles in adipose tissue and obesity [12]. Specifically, there are also increasing evidence of the role of lncRNAs in adipogenesis, where their expression levels correlate with different stages of adipocytes differentiation, they can regulate key players in adipogenesis (e.g., PPARγ), or even associate with adipogenesis-implicated miRNAs [13,14]. Moreover, RNA-seq screening allowed the identification of deregulated targets in patients with obesity or murine models of obesity [15,16]. These studies have been performed in both brown and white adipose tissue, providing reference of a number of adipogenesis-related lncRNAs [15,17]. Hence, lncRNAs are emerging as new potential candidate targets for therapeutic development as well as comorbidities regulators [16,18–21].

In this framework, the aim of this work was the characterization of transcriptional differences in the subcutaneous adipose tissue (SAT) of obesity-affected versus normal weight healthy women. We previously highlighted the presence of different transcriptional profiles in obesity-affected men and women, highlighting gender-specific differences in transcription, and we also performed a characterization of the oncogenic susceptibility present in SAT tissues of normal weight subject, obesity-affected women, obesity and type 2 diabetes-affected women and obesity-affected men [4,22]. We now aim to perform an in-depth characterization of coding and non-coding transcripts in obesity-affected women versus healthy women, specifically focusing on role of the deregulated lncRNAs. Here we investigate a panel of them (n = 6) in terms of expression and regulation in human Adipose Derived Stem Cells (hADSCs) differentiation to adipocytes.

2. Materials and methods

2.1. Adult human adipose tissue collection, isolation and differentiation

The present study is in accordance with the Declaration of Helsinki, and it was approved by the Ethical Committee of IRCCS Istituto Auxologico Italiano (Ethical Committee approval code #2020_10_20_04). A signed informed consent was obtained from each enrolled patient for tissue sampling. Biopsies of SAT were collected from a total of 10 subjects: 5 healthy CTRL women (age 37 ± 6.7 years, BMI 24.3 ± 0.9 kg/m2) and 5 women with obesity (age 41 ± 12.5 years, BMI 38.2 ± 4.6 kg/m2). Patients were chosen so not to have significant differences amongst groups which could impact on gene expression (Table S1). Surgical biopsies of whole abdominal SAT were collected pre-operatively from obese patients during bariatric surgery procedures and from CTRL women before aesthetic plastic surgery or abdominal surgery for non-inflammatory diseases. Each collected biopsy was weighed and stored in 1 mL of DMEM (Invitrogen Corporation, Jefferson City, MO) supplemented with 2.5% Bovine Serum Albumin (Sigma, St. Louis, MO) per gram of collected tissue. The biopsy was immediately transferred to the laboratory and processed. A fragment of the whole adipose tissue biopsy was immediately frozen in liquid nitrogen for RNA extraction (see below), another fragment was formalin-fixed, and the remaining material was digested with 1 mg/mL collagenase type 2 (Sigma, St. Louis, MO) for at least 1 h at 37 °C under shaking. The digested tissue was then filtered through a sterile gauze and a nylon filter (BD Bioscience 1 Becton Drive Franklin Lakes, NJ). The SVF cells were isolated by centrifugation and then treated with a buffer containing 154 mM NH4Cl, 10 mM KHCO3, and 0.1 mM EDTA for lysis of red blood cells. Stroma-Vascular Fraction cells were plated and cultured in a medium containing a 1:1 mixture of Ham's F12/DMEM (Invitrogen Corporation, Jefferson City, MO) supplemented with 10% Fetal Bovine Serum (FBS, Sigma, St. Louis, MO) until confluence. The cells obtained have been identified to be human Adipose Derived Stem Cells [23]. At confluence, cells were differentiated into mature adipocytes using AdipoStemPro (Invitrogen) for 10 days.

2.2. SAT RNA extraction

Approximately 500 mg of frozen SAT was homogenized in RLT buffer (Qiagen). RNA from SAT was extracted using the RNeasy Mini Kit (Qiagen) according to the manufacturer protocol and samples were then treated with the RNase-Free DNase Set (Qiagen). Concentration and quality of the extracted RNA were determined by the NanoDrop ND-1000 spectrophotometer (NanoDrop Technologies, USA) and RNA integrity verified by gel-electrophoresis.

2.3. RNA-Seq and bioinformatic data analysis

RNA-seq analysis was performed on one replicate for each SAT biopsy (5 healthy CTRL women and 5 women with obesity). RNA-seq libraries were prepared with the CORALL Total RNA-Seq Library Prep Kit (Lexogen, Vienna, Austria) using 150 ng total RNAs. The RiboCop rRNA Depletion Kit (Lexogen, Vienna, Austria) was used to remove rRNA. Qualities of sequencing libraries were assessed with D1000 ScreenTape Assay using the 4200 TapeStation System (Agilent, Santa Clara, CA, USA) to account for variability in library quality and quantified with Qubit™ dsDNA HS Assay Kit (Invitrogen, Carlsbad, CA, USA). To account for technical variability in library dimension the single libraries were normalized for their molarity using the respective “library quantification file” (Lexogen, Vienna, Austria) which calculates the molarities of each library from the concentration measurement and average size, providing the volumes of each library to be used for preparation of an equimolar lane mix.

RNA processing was carried out using Illumina NextSeq 500 Sequencing. FastQ files were generated via llumina bcl2fastq2 (v. 2.17.1.14; https://support.illumina.com/downloads/bcl2fastq-conversion-software-v2-20.html, last accessed on 15 February 2021) starting from raw sequencing reads produced by Illumina NextSeq sequencer. Quality of individual sequences was evaluated using FastQC software (see Code Availability 1) after adapter trimming with cutadapt software. Transcript abundance was obtained using the BlueBee® Genomics Platform (Lexogen, Vienna, Austria) using Gencode Release h38 (GRCh38) as a reference. Differential expression analysis was performed using R package DESeq2, which contains a further library normalization step. Genes were considered differentially expressed and retained for further analysis with $|\log2(\text{condition sample/control sample})| \geq 1$ and

a False Discovery Rate (FDR) ≤ 0.1. The raw data obtained from the RNA-seq analysis are deposited in the Gene Expression Omnibus repository with the accession number GSE166047. The expression of a panel of genes with relevant FC differences was previously analyzed via Real-Time PCR in technical duplicates in an independent cohort of SAT samples obtained from normal-weight females and females affected by obesity. This accounts for technical and inter-individual differences [4].

2.4. Pathway analysis

Gene set enrichment analysis was performed on clusterProfiler R package [24]. Gene set from Molecular Signature databases such as curated gene set (C2) and ontology gene sets (C5) and a p value cut off <0.05 were considered for this analysis [24]. The R software was used to generate heatmaps (*heatmap.2* function from the R *ggplots* package), PCA plot (*prcomp* function from the R *ggplots* package), and Volcano plots [25]. The NDEx plugin [26] was used to perform analysis regarding the subcellular localization of the differentially expressed genes [27].

2.5. Coding and ncRNAs co-expression analysis

Coding RNAs' co-expression with ncRNAs was performed using Weighted gene co-expression network analysis (WGCNA) R package (https://CRAN.R-project.org/package=WGCNA) [28]. The soft thresholding power was chosen considering the criterion of approximate scale-free topology. Network nodes represent gene expression profiles, while undirected edges values are the pairwise correlations between gene expressions. Cytoscape software was used for network import and visualization.

2.6. In silico dissection of lncRNAs

The AnnoLnc2 database was used for characterization of each lncRNA [29]. The FASTA sequence for each lncRNA was submitted to the website, which retrieved information on the lncRNAs localization, repeat elements analysis through the RepeatMasker genomic datasets, sequence conservation with PhyloP, PhastCons scores and Derived Allele Frequency (DAF) scores, lncRNAs expression, localization, and localization motifs. The secondary structure prediction was used for the identification of miRNA and protein binding sites (identified via CLIP-Seq). Moreover, AnnoLnc2 through GTRD database allowed to highlight peak clusters of transcription factors (TFs) in adipocytes, and we also cross-referenced all the genes which emerged as positively correlated with each lncRNA with the DE RNAs from our RNA-seq analysis. Amongst these, we searched for cis/trans correlations with the LncEXPdb [30] interaction section. Lastly, we investigated the biological processes positively correlated with the AnnoLnc2 database and we report the top 20 significant pathways.

2.7. hADSCs' isolation

Primary cell cultures from normal weight human adipose tissue samples were obtained from one volunteer healthy subject undergoing elective liposuction procedures under local anesthesia. Briefly, cells were isolated after directly plating the pellet without centrifugation in complete DMEM prepared with DMEM (Euro Clone) containing 1 g/L D-glucose 10% heat-inactivated FBS supplemented with antibiotics at 37 °C in a humidified, 5% CO_2 incubator (HERA cell 150- Thermo electron, USA). The obtained cells were characterized for their karyotype and immunophenotype [31,32]. All cell cultures were maintained at 37 °C in humidified atmosphere containing 5% CO_2. After 2 weeks, the non-adherent fraction was removed and the adherent cells were cultured continuously, while the medium was changed every 3 days.

2.8. Adipogenic induction

hADSCs were differentiated in adipogenic medium composed of DMEM High Glucose (Euroclone) supplemented with 10% Fetal Bovine Serum (GIBCO™), antibiotics (1% Penicillin/Streptomycin, 0.3% Amphotericin B) (Euroclone), 1% L-Glutamine (Euroclone), 1 μmol/L dexamethasone (Sigma-Aldrich), 0.5 mM 3-isobutyl-1-methyl-xanthine (Sigma-Aldrich), 10 μM insulin (Sigma-Aldrich) and 200 μM indomethacin (Sigma-Aldrich). The medium was changed every 3 days. In the experiments showed in this work adipogenic induction required 7 days [31,33,34], but time-point experiments were also conducted assessing adipogenic differentiation at different days.

2.9. Pharmacological treatments

PPARγ was activated using the ligand agonist troglitazone [35,36]. 1 μg/mL troglitazone (Sigma-Aldrich) was added to the standard culture medium with 10% FBS for 7 days, and medium was changed every 2 days. PPARγ was inhibited with the selective PPARγ antagonist T0070907 (Sigma-Aldrich) [37]. 1 μM of T0070907 was added to the standard culture medium for 7 days, and the medium was changed every 2 days [34].

2.10. Gene expression silencing

RNA interference was used to suppress specific gene expression. Briefly, two days before transfection, 6000 cells/cm^2 were plated in standard growth medium. Transfection was performed with Lipofectamine® RNAiMAX Reagent (Thermo Fisher) and siRNA agent. This was a siRNA mock (Silencer™ Select Negative Control No. 1 siRNA-Cat # 4390843, Thermo Fisher) or the siRNA for the respective target (Silencer Select pre-designed siRNA for C/EBPα-s532363, C/EBPδ - s2894, C/EBPβ - s63860 and CTEPHA1 - n360183; Thermo Fisher) diluted in the appropriate volume of Opti-MEM® Medium (Thermo Fisher). Samples were incubated for <15 min at room temperature and the siRNA-lipid complex was gently dropped in the wells containing the cells, which were then incubated for 72 h days at 37 °C in a CO_2 incubator.

2.11. Real Time PCR

Total RNA was isolated using TRIzol Reagent ™ (Invitrogen) in accordance with manufacturer's instructions. 500 ng of RNA were reverse transcribed using the iScript ™ Reverse Transcription Supermix for RT-qPCR (Bio-Rad). Real Time PCR was performed with StepOnePlus™ Real Time PCR System (Thermo Fisher) using Sso SYBR Green Supermix (Bio-Rad). Samples were analyzed with the $2^{-\Delta\Delta Ct}$ method, where ΔΔCt = ΔCt sample – ΔCt reference (38). Primers were designed using human gene sequences available from NCBI (www.ncbi.nlm.nih.gov/nucleotide), and selected using NCBI's Primer- BLAST tool at the exon junctions' level to optimize amplification from RNA templates and avoiding nonspecific amplification products. Primers were designed to have a sequence of about 20 bp and perform a PCR product size of maximum 250 bp. 18S and GAPDH were used as housekeeping genes. Primer used are shown in Table S2.

2.12. Statistical analysis

Statistics was evaluated using GraphPad Prism 8.0a version (GraphPad Software Inc., La Jolla, USA). When two conditions were analyzed, Student's unpaired *t*-test was used. When three or more conditions were analyzed, one-way ANOVA was used followed by Tukey's post-test. For all in vitro experiments, data are reported as mean ± Standard Error Mean (SEM). The level of statistical significance was set at p = 0.05.

3. Results

3.1. Obesity alters expression profiles of coding and non-coding genes in SAT

Subcutaneous adipose tissue (SAT) from 5 normal weight women (CTRL) and 5 women affected by obesity (OBF), were compared in order to analyze the transcriptional differences present at tissue level.

RNA-sequencing analysis was performed with a cluster density of 174 K/mm^2 and a cluster passing filter was 90.4%, indicating that the raw data obtained was in line with the expected values required for subsequent analyses. When filtering for transcripts with >20 reads, 30,327 total variables were identified, 18,674 of which were coding genes and 11,653 of which were non-coding transcripts. Specific details on library quality are reported in our Data in Brief report (unpublished data, under review).

After RNA-Seq analysis, genes were analyzed according to their Fold Change (FC) and their False Discovery Rate (FDR). Genes showing $|\log2FC| \geq 1$ and an FDR ≤ 0.1 were considered as differentially expressed (DE RNAs). The differentially expressed genes were represented as heatmap (Fig. 1A), and clustering analysis showed that OBF and CTRL clearly separated. Moreover, a volcano plot was built considering a total of 60,199 genes and it reports the dysregulation profile between OBF vs CTRL (Fig. 1B). Specifically, a total of 171 DE RNAs were detected in SAT tissue from OBF versus CTRL (Table 1). Of these, 160 were coding genes (mRNAs; 127 up-regulated DE RNAs and 33 down-regulated DE RNAs) and 11 were non-coding genes (ncRNAs; 8 up-regulated DE RNAs and 3 down-regulated DE RNAs).

The sub-type characterization of the ncRNAs is reported in Table 2 with a classification of these ncRNAs for their specific biotype. It is possible to observe how the most abundant category are Natural Antisense Transcripts (NATs), followed by long intergenic non-coding RNAs (lincRNAs), both lncRNAs. As NATs and lincRNAs are the most abundant category of differentially expressed ncRNAs, we decided to focus on the role of lncRNAs for all further experiments and analyses.

A bibliographic analysis of previous literature was performed, in order to identify how many, amongst the 171 DE RNAs had been previously associated with obesity (Fig. 1C). Almost half of the deregulated genes (47.37%) had never been associated with the obesity condition and moreover, most of the studies concerning the 90 obesity-associated genes were observational studies, correlating the genes to an obese phenotype (Fig. 1C).

3.2. Role of the non-coding transcriptome in SAT from obese patients

The several non-coding DE RNAs that emerged as differentially expressed are reported as a volcano plot graph highlighting only the non-coding component (Fig. 1D). Out of the 11 deregulated DE RNAs which emerge from transcriptional analysis of OBF vs. CTRL SAT, 6 belong to the lncRNAs category (Table 3). Most are uncharacterized genes, with unknown function, and interestingly three of them are NATs to coding genes (COL4A2, ITGB2, and RPS21). The common aliases for each will be used for now on: PELATON, COL4A2-AS2, CTEPHA1, RPS21-AS, ITGB2-AS1, ACER2-AS.

A study of the coding/non-coding components interaction was done performing a WGCNA analysis, and the obtained network with a weighted correlation threshold of 0.1 is reported in Fig. 1E. Specifically 8 ncRNAs emerge as part of the interactome and 6 of these are lncRNAs (reported in pink). RPS21-AS, CTEPHA1, and ITGB2-AS1 form three independent networks, whereas COL4A2-AS2, SMIM25 and ACER2-AS all take part in a main coding/non-coding correlation network (Fig. 1E).

3.3. In silico characterization of 6 DE lncRNAs

We then decided to perform a specific computational dissection of each lncRNA in order to shed a preliminary light on their possible function in the adipose tissue and in obesity. An in detail dissection of all analyses performed is reported for COL4A2-AS2. COL4A2-AS2 is an antisense lncRNA to COL4A2, localized on the – strand of Chromosome 13 (Fig. S1A). Its sequence was analyzed with the AnnoLnc2 database for further characterization. Repeat elements analysis through the RepeatMasker genomic datasets highlighted the presence of only one repeat element, MLT1C (of the LTR/ERVL-MaLR repeat class) (Table S3). We analyzed its sequence conservation with PhyloP and PhastCons scores, aimed at assessing base conservation amongst species (Fig. S1B). PhyloP analysis highlights a tendency for fast evolution for exon sequences and a reduced conservation for promoter sequences. Conversely, PhastCons also indicates that the conservation score is not in the range of "conserved sequences", especially in primates, for both exon and promoter sequences. Derived Allele Frequency (DAF) score is around 0.35, suggesting that the gene is not under strong purifying selection. Moreover, we assessed its expression profile and found that COL4A2-AS2 is expressed mainly in the adipose tissue, blood vessels and nerves (Fig. 2A). Analysis of localization motifs indicated the presence of nuclear-localization domains, although analysis of localization from nuclear and cytosolic RNA-seq samples of 10 cell lines from ENCODE indicated a cytoplasmic localization for the lncRNA (Fig. S1C, Table S4). The secondary structure prediction could be useful in the identification of miRNA (Fig. S1D and Table S5) and protein binding sites (identified via CLIP-Seq, Fig. S1E and Table S6), which could modulate the lncRNAs expression and mechanism of action. AnnoLnc2 through GTRD database allowed to highlight peak clusters of transcription factors (TFs) in adipocytes, and these specifically are CTCF, PPARG and RELA (Table S7). We also cross-referenced all the genes which emerged as positively correlated with COL4A2-AS2 with the DE RNAs from our RNA-seq analysis and found that there were no matches in this case (Fig. S1F). Lastly, we investigated the biological processes positively correlated with this lncRNAs and we report the top 20 significant pathways in Fig. 2B. Remarkably the most significant pathway pertained +ve regulation of fat cell differentiation, and other relevant processes include "regulation of cellular response to insulin stimulus" and "regulation of fat cell differentiation".

RPS21-AS (AL121832.2) is also localized on Chromosome 20, on the – strand, opposite to RPS21, a ribosomal protein (Fig. S2A). It presents a LINE repeat element (Table S3), its exon appears fast evolving and under strong purifying selection, differently from the promoter (Fig. S2B), and it has a ubiquitary expression (mainly in the testis, Fig. 2C). It presents a nuclear motif (Table S4) but localizes in the cytosol in 7/10 studied cell lines (Fig. S2C), it presents binding sites for 19 miRNAs (Fig. S2D and Table S5), has 87 interactions with proteins (Fig. S2E and Table S6) and it is modulated by KLF11, CTCF and PPARG in adipocytes (Table S7). It has 3883 positively correlated genes, none present amongst our DE RNAs, and it correlates with response to stimulus, sexual reproduction and male gametes (Fig. 2D).

PELATON is localized on the + strand of Chromosome 20 (Fig. S3A), it presents repeat elements of the SINE and LINE class (Table S3) and its sequence does not appear to be highly conserved, although its promoter is under strong purifying selection (Fig. S3B). It presents nuclear localization binding motifs (Table S4) but it localizes in the cytoplasm in HeLa cells (Fig. S3C) and it is mainly expressed in the blood, lung, spleen and adipose tissue (Fig. 3A). It is predicted to interact with 70 miRNA (Fig. S3D and Table S5), it is bound by FUS (Fig. S3E and Table S6) and it is regulated by 5 TFs in adipocytes (PPARG, CTCF, RELA and EP300, Table S7). Amongst the 639 positively correlated genes, 15 are DE RNAs from our datasets, and for two of them, DOK3 and TYROBP, a *trans* regulation has been found (LncEXPdb, Fig. 3B). Moreover, it positively correlates with immunogenic processes (Fig. 3C).

ITGB2-AS1 localizes on the + strand on Chromosome 21, antisense to ITGB2 (Fig. S4A). It presents a LINE and a single repeat (Table S3), it does not appear to be strongly conserved nor under strong purifying selection (Fig. S4B) and no data is currently present on its localization, though it is enriched mainly in the blood, lung, and spleen (Fig. 3D). It

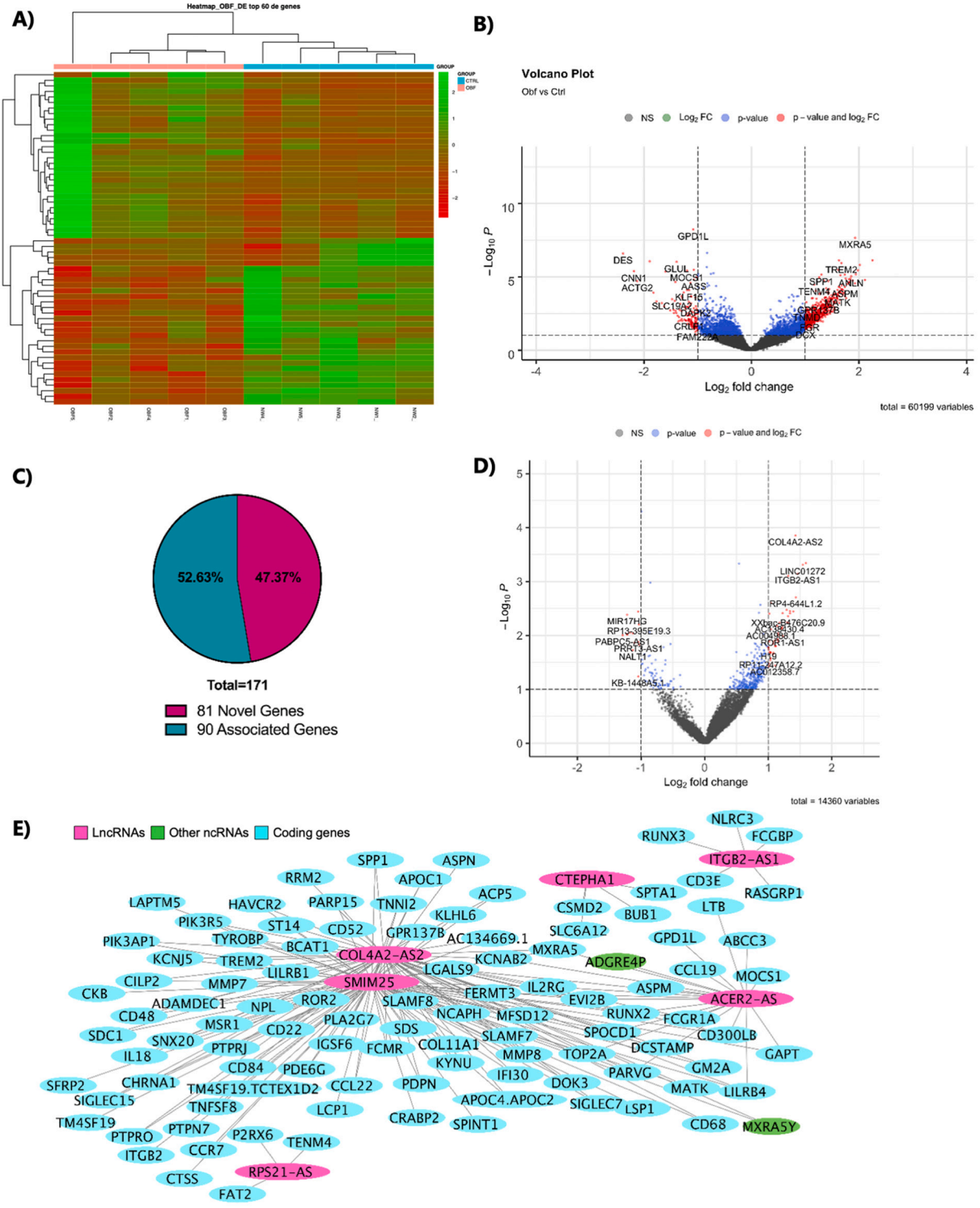

Fig. 1. Global transcriptional deregulation in coding and non-coding genes is present in SAT from OBF and CTRL. (A) Expression profiles of differently expressed genes in OBF versus CTRL reported as a Heatmap. (B) Volcano plot showing deregulated genes between OBF and CTRL. On the x axis is reported the $\log_2$FC whereas on the y axis is reported the P value in logarithmic scale. (C) pie chart of genes previously associated with obesity. (D) Volcano plot showing deregulated non-coding genes between OBF and CTRL. On the x axis is reported the $\log_2$FC whereas on the y axis is reported the P value in logarithmic scale. (E) WGCNA of OBF vs. CTRL highlighting lncRNAs. The correlation threshold was set to 0.1 and the lncRNAs are reported in pink, whilst other ncRNAs are reported in green. The thicker edges refer to the first-degree interactions of non-coding DE RNAs. (For interpretation of the references to color in this figure legend, the reader is referred to the web version of this article.)

Table 1
Number of differentially expressed genes in the SAT of OBF vs. CTRL.

	OBF vs. CTRL		
	mRNAs	ncRNAs	Total
Up Regulated	127	8	135
Down Regulated	33	3	36
Total	160	11	171

Table 2
Biotype characterization of differentially expressed ncRNAs. TEC: To be Experimentally Confirmed; IG C pseudogene:inactivated immunoglobulin gene.

	ncRNAs		
	Up Regulated	Down Regulated	Total
NATs	3	1	4
lincRNAs	2	0	2
Processed pseudogene	0	1	1
TEC	0	1	1
Transcribed unprocessed pseudogene	1	0	1
IG_C_pseudogene	1	0	1
Unprocessed pseudogene	1	0	1
Total	8	3	11

Table 3
List of lncRNAs DE in OBF vs CTRL SAT.

Gene_name	Log2FC	Aliases	Function
COL4A2-AS2	5.93		NAT to COL4A2, which pays a role in osteogenic differentiation and is differentially secreted in adipogenic differentiation.
SMIM25	2.74	GCRL1, LINC01272, PELATON	Nuclear expressed, monocyte- and macrophage-specific lncRNA, upregulated in unstable atherosclerotic plaque.
AL121832.2	2.36	RPS21-AS	NAT to RPS21, unknown function
ITGB2-AS1	2.23		NAT to ITGB2 and polymorphism in ITGB2 were associated with obesity.
LINC01094	1.74	CTEPHA1	Deregulated in post-menopausal osteoporosis, implicated in Chronic Thromboembolic Pulmonary Hypertension
AL158206.1	−1.07	ACER2-AS	NAT to ACER2, an alkaline ceramidase implicated in lipids metabolism.

presents 78 miRNA (Fig. S4C and Table S5) binding sites, it is also bound by FUS (Fig. S4D, Table S6) and presents binding sites in adipocytes for CEBPA, CTCF, LMNA, MBD4, PPARG and RELA (Table S7). It positively correlates with 421 genes, amongst them 7 are DE RNAs, and specifically with EVI2B and CTSS it was found to interact in *trans* (LncEXPdb, Fig. 3E) and it also appears implicated in immunogenic processes (Fig. 3F).

ACER2-AS (AL158206.1) localizes on the + strand of Chromosome 9, antisense to ACER2 (Fig. S5A), it presents two single repeats (Table S3), it appears to be more conserved than fast evolving (especially its exon, Fig. S5B), it localizes in the cytosol in 6/10 analyzed cell lines but presents nuclear retention motives (Fig. S5C and Table S4) and it is mainly enriched in the adipose tissue (Fig. 4A). It has binding sites for 60 miRNAs (Fig. S5D and Table S5), 69 proteins (Fig. S5E and Table S6) and PPARG in SAT (Table S7). Out of the 14 positively correlated genes there are ACER2-AS itself and ACER2, both DE RNAs (Fig. 4B), and the RNA appears implicated in Acyl-CoA biosynthetic processes (Fig. 4C).

The last DE ncRNA is CTEPHA1, localized on the + strand of Chromosome 4 (Fig. S6A), with 7 repeat elements (Table S3), it appears to be rather conserved (Fig. S6B), with a cytoplasmic localization (Fig. S6C, although a nuclear motif, Table S4) and a predominant expression in the blood and vagina (Fig. 4D). The binding sites for miRNAs, proteins and TFs in adipocytes are respectively 145 (Fig. S6D and Table S5), 1 (Fig. S6E and Table S6) and 10 (Table S7, with CEBPA amongst them). It is positively correlated with 7 DE RNAs (Fig. 4E) and it is involved in immune system processes (Fig. 4F).

3.4. LncRNAs present time-point specific deregulation during adipogenic differentiation

As our RNA-seq highlighted that these lncRNAs have been found to be deregulated in SAT of obese patients, in vitro differentiation experiments were performed to investigate their role in adipogenesis, both in obesity-affected patients and in healthy subjects. We firstly analyzed the expression of the 6 lncRNAs in SAT mesenchymal stem cells from obese patients, along with the sense genes RPS21 and COL4A2, in order to assess whether dysfunctions observed at whole tissue level were also recapitulated during adipogenic processes in obesity affected patients. Cells were differentiated for 14 days under standard adipogenic differentiation protocol and all of the lncRNAs present changes in expression along different phases of differentiation (Fig. 5A, Fig. S7A). Interestingly, in the case of CTEPHA1, ITGB2-AS1 and COL4A2-AS2, the expression seems to initially decrease, in a divergent manner to that of SAT from obesity-affected women, and this indicates the genes could act differently at whole tissue level as opposed to cellular differentiation. The other genes present an increase during adipogenic differentiation. The genes expression was also analyzed during the differentiation of hADSCs obtained from the lipoaspirate of a healthy subject used as control (CTRL), in order to assess whether these lncRNAs could also play a role in adipogenesis of healthy subjects (Fig. 5B, Fig. S7B). Also, in this case the expression of the lncRNAs and sense genes changes at the different phasis of the adipogenesis process, and they all seem to present a peak at day 7, with the highest significance for PELATON, RPS21-AS, CTEPHA1, COL4A2 and RPS21 (Fig. 5B, Fig. S7B). Interestingly, in the case of CTEPHA1, ITGB2-AS1, PELATON, COL4A2-AS2 and COL4A2, the expression seems to peak at day 7, with a subsequent decrease. On the contrary, for ACER2-AS, RPS21-AS and RPS21, the increase seems to be constant and maintained up to day 14 (Fig. 5B, Fig. S7B). Moreover, the pattern of sense/antisense genes is not necessarily concordant, but this is in line with reports highlighting a function for antisense gene in both positive regulation and inhibition of sense genes expression [39].

3.5. LncRNAs can be selectively modulated by adipogenesis-related transcription factors

As there is a time-point specific alteration of the lncRNAs expression we investigated whether this could be due to adipogenesis-TFs regulation, as these lncRNAs present TFs binding sites in their promoter sequence (Table S7). We thus decided to modulate the expression of C/EBPβ, C/EBPδ, C/EBPα and PPARγ, as these are known TFs regulating adipogenesis. To do so, we silenced the expression of the C/EBPs via RNA interference (Figs. 6A–C, Fig. S8A–C). Specifically, we found that C/EBPβ significantly influenced RPS21-AS, ITGB2-AS1, ACER2-AS and CTEPHA1 (Fig. 6A), whereas PELATON, ITGB2-AS1, ACER2-AS and CTEPHA1 were significantly reduced when the expression of C/EBPδ was decreased (Fig. 6B) and lastly PELATON, ITGB2-AS1 and CTEPHA1 were decreased by C/EBPα inhibition (Fig. 6C). As PPARγ is known to be adipogenesis' master regulator [40,41], its influence on the investigated lncRNAs and respective sense genes was analyzed. To do so, its activity was induced with the pharmacological activator troglitazone in undifferentiated conditions [34], whilst we inhibited it with the inhibitor T0070907 administered during adipogenic differentiation (Fig. 6D, Fig. S8D). COL4A2-AS2, PELATON and CTEPHA1 were induced by PPARγ's activation, whilst ITGB2-AS1 appears to be inhibited by it (conversely with its trend during differentiation). Moreover, all the lncRNAs were induced during differentiation except for ITGB2-AS1, which was decreased. The treatment with the PPARγ inhibitor did not appear to influence their expression (Fig. 6D).

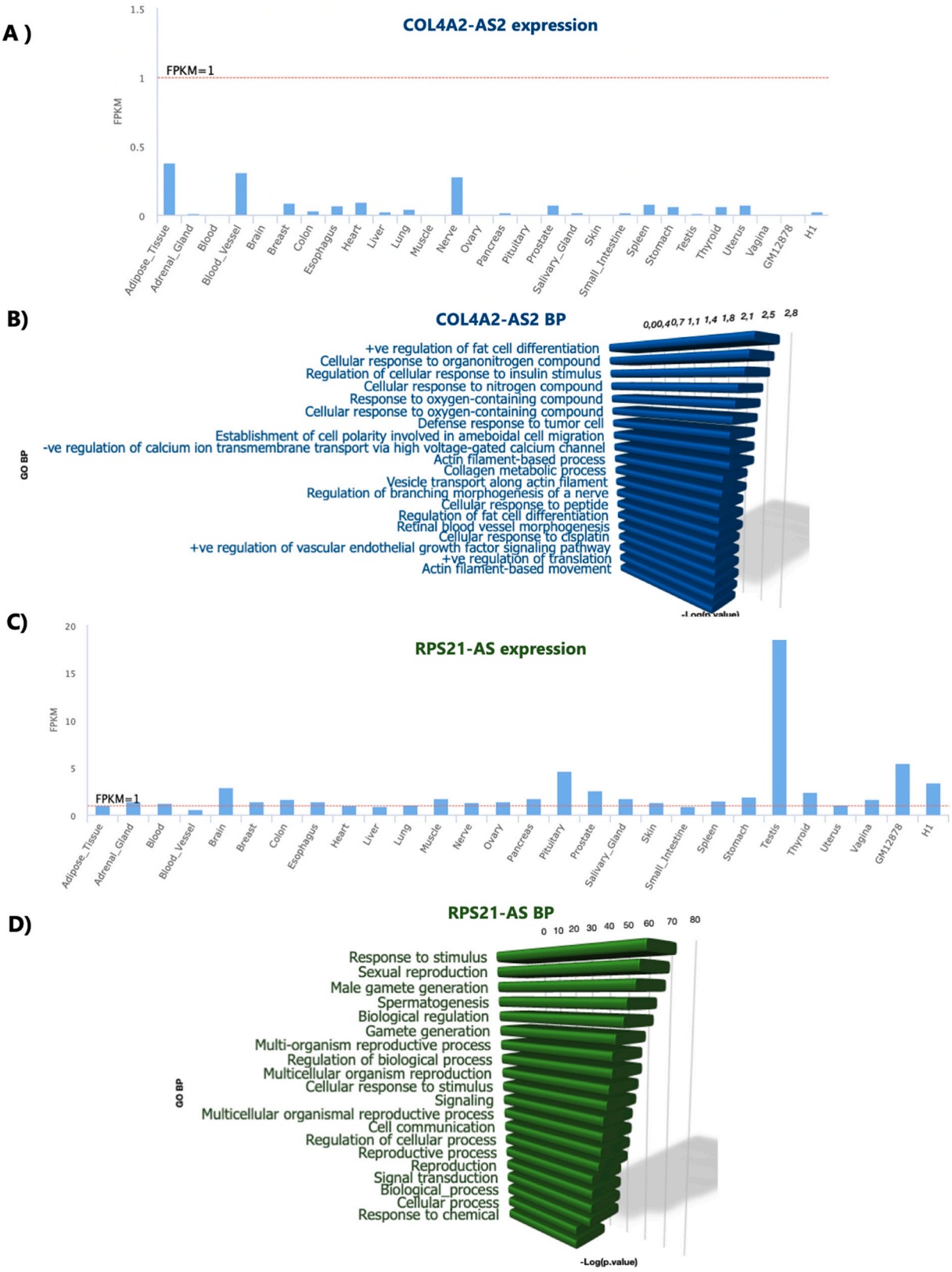

Fig. 2. In silico dissection of COL4A2-AS2 and RPS21-AS. (A) Tissue expression data of COL4A2-AS2 as obtained with AnnoLnc2 database (B) BP of the pathways positively correlated with COL4A2-AS2 in normal tissue obtained with the AnnoLnc2 database and reproduced as bar plot graph. On the Y axis the pathway name, on the x axis the -log(p.value) of the pathway. (C) Tissue expression data of RPS21-AS as obtained with AnnoLnc2 database (D) BP of the pathways positively correlated with RPS21-AS in normal tissue obtained with the AnnoLnc2 database and reproduced as bar plot graph. On the Y axis the pathway name, on the x axis the -log(p. value) of the pathway.

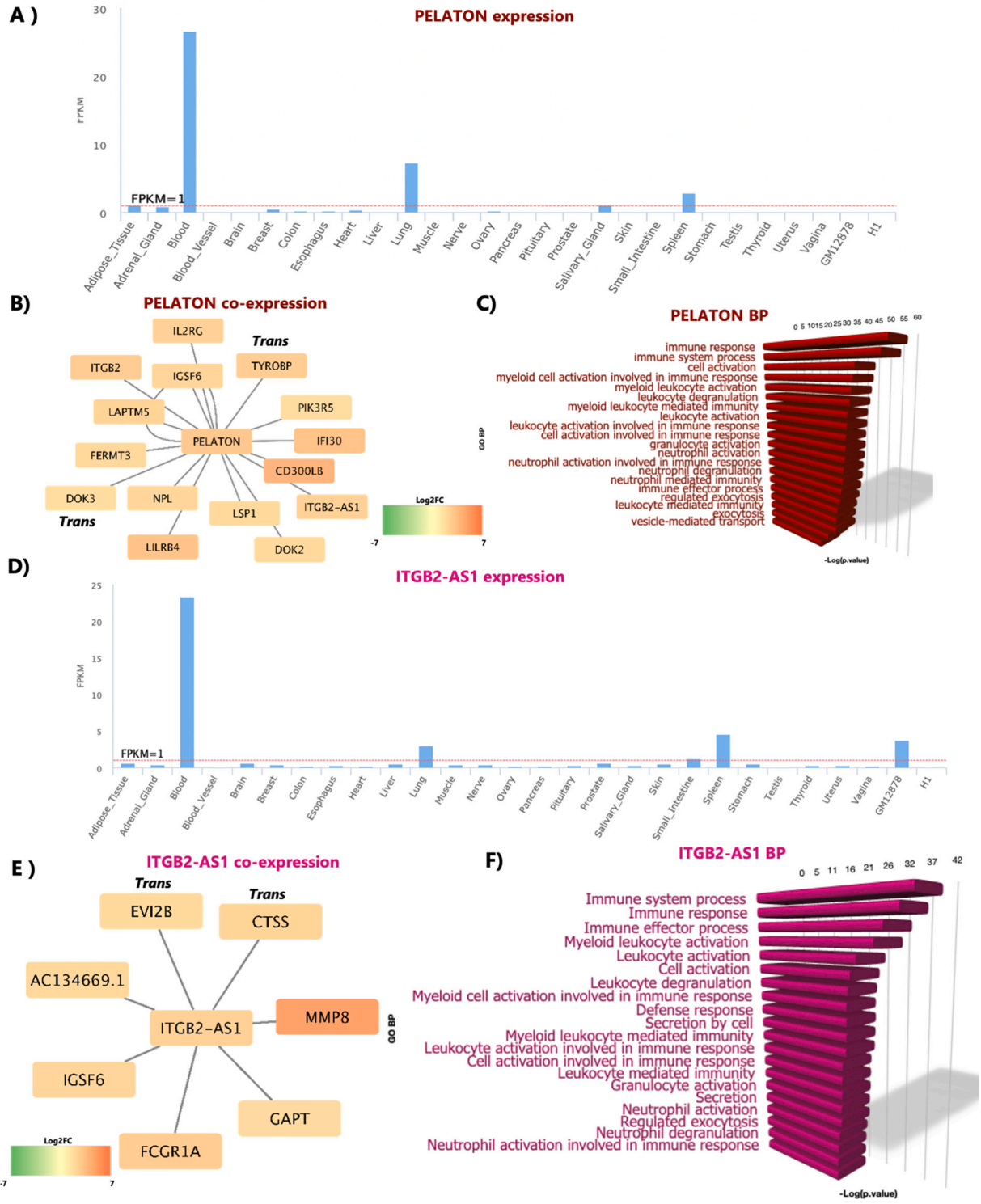

Fig. 3. In silico dissection of PELATON and ITGB2-AS1. (A) Tissue expression data of PELATON as obtained with AnnoLnc2 database (B) Network of genes positively correlated with PELATON present in the AnnoLnc2 database cross-referenced with the DE RNAs present in this dataset. The LncEXPdb was used to identify potential correlation in cis and trans, which when present are reported on the graph. The network was built with Cytoscape and the color scale refers to the genes expression in terms of Log2FC (C) BP of the pathways positively correlated with PELATON in normal tissue obtained with the AnnoLnc2 database and reproduced as bar plot graph. On the Y axis the pathway name, on the x axis the -log(p.value) of the pathway. (D) Tissue expression data of ITGB2-AS1 as obtained with AnnoLnc2 database (B) Network of genes positively correlated with ITGB2-AS1 present in the AnnoLnc2 database cross-referenced with the DE RNAs present in this dataset. The LncEXPdb was used to identify potential correlation in cis and trans, which when present are reported on the graph. The network was built with Cytoscape and the color scale refers to the genes expression in terms of Log2FC (D) BP of the pathways positively correlated with ITGB2-AS1 in normal tissue obtained with the AnnoLnc2 database and reproduced as bar plot graph. On the Y axis the pathway name, on the x axis the -log(p.value) of the pathway.

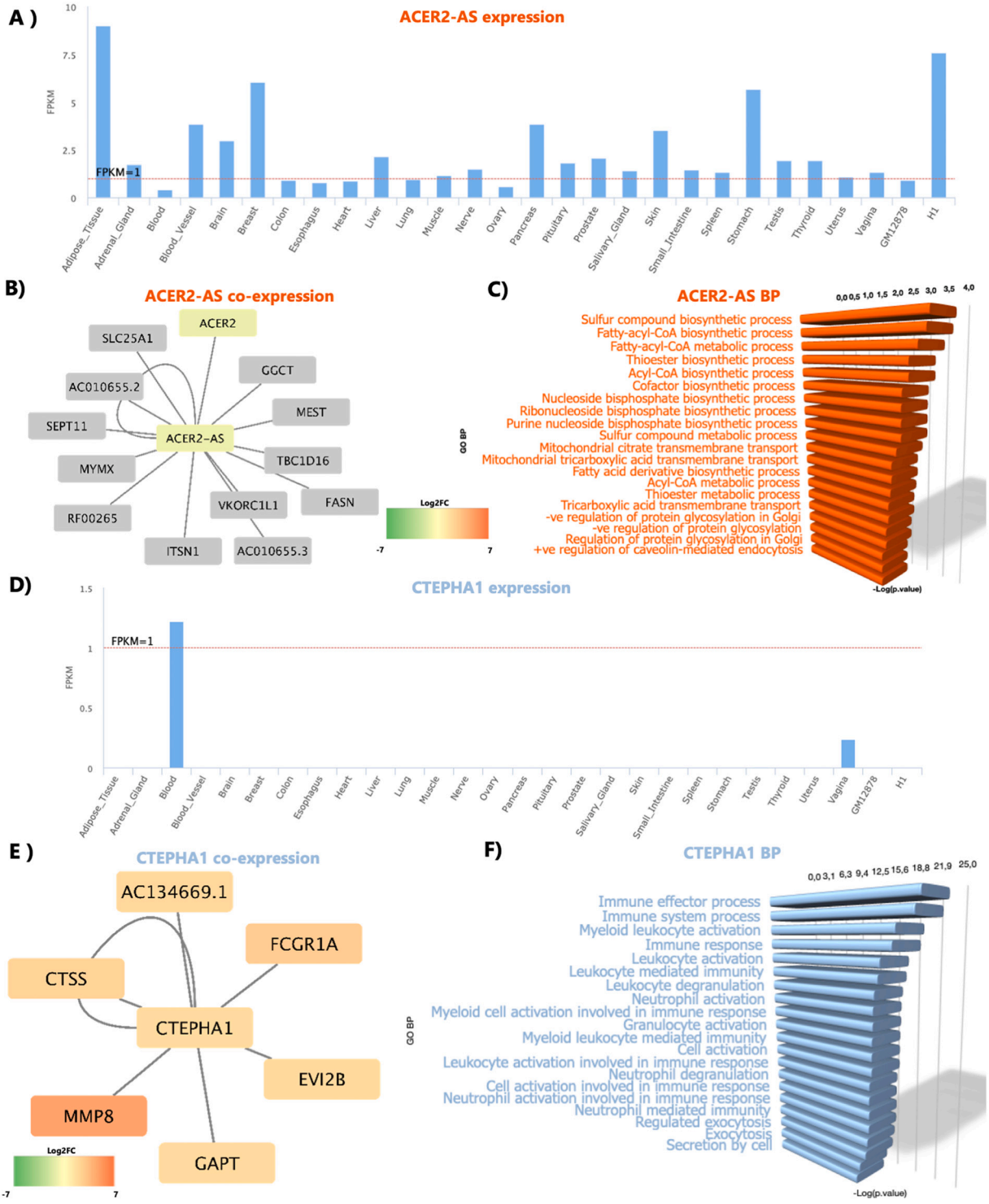

Fig. 4. In silico dissection of ACER2-AS and CTEPHA1. (A) Tissue expression data of ACER2-AS as obtained with AnnoLnc2 database (B) Network of genes positively correlated with ACER2-AS present in the AnnoLnc2 database cross-referenced with the DE RNAs present in this dataset. The LncEXPdb was used to identify potential correlation in cis and trans, which when present are reported on the graph. The network was built with Cytoscape and the color scale refers to the genes expression in terms of Log2FC (C) BP of the pathways positively correlated with ACER2-AS in normal tissue obtained with the AnnoLnc2 database and reproduced as bar plot graph. On the Y axis the pathway name, on the x axis the -log(p.value) of the pathway. (D) Tissue expression data of CTEPHA1 as obtained with AnnoLnc2 database (B) Network of genes positively correlated with CTEPHA1 present in the AnnoLnc2 database cross-referenced with the DE RNAs present in this dataset. The LncEXPdb was used to identify potential correlation in cis and trans, which when present are reported on the graph. The network was built with Cytoscape and the color scale refers to the genes expression in terms of Log2FC (D) BP of the pathways positively correlated with CTEPHA1 in normal tissue obtained with the AnnoLnc2 database and reproduced as bar plot graph. On the Y axis the pathway name, on the x axis the -log(p.value) of the pathway.

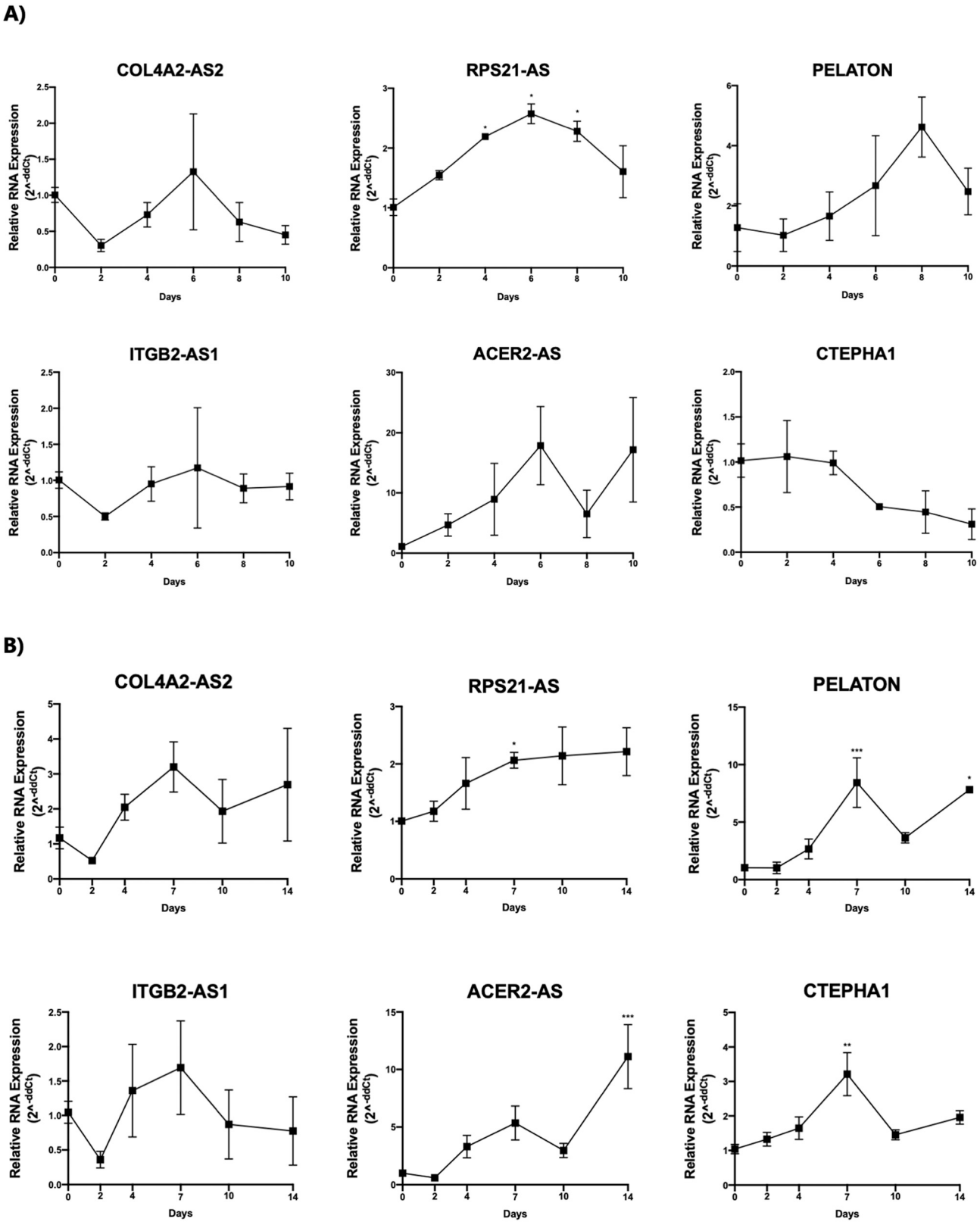

Fig. 5. LncRNAs expression during adipogenic differentiation of ADSCs of normal weight and obese subjects. (A) Differential expression of lncRNAs in adipocytes obtained from SAT tissue from obese patients was verified by Real Time PCR. 18S was used as housekeeping gene. Data are expressed as mean of 2 samples ± SEM (n = 2), *p < 0.05 vs. SAT Day 0. (B) Differential expression of lncRNAs in lipoaspirate of a CTRL subject was verified by Real Time PCR. GAPDH was used as housekeeping gene. Data are expressed as mean of 3 experiments each performed in duplicates ± SEM (n = 6), *p < 0.05, **p < 0.01, ***p < 0.001 vs. Day 0.

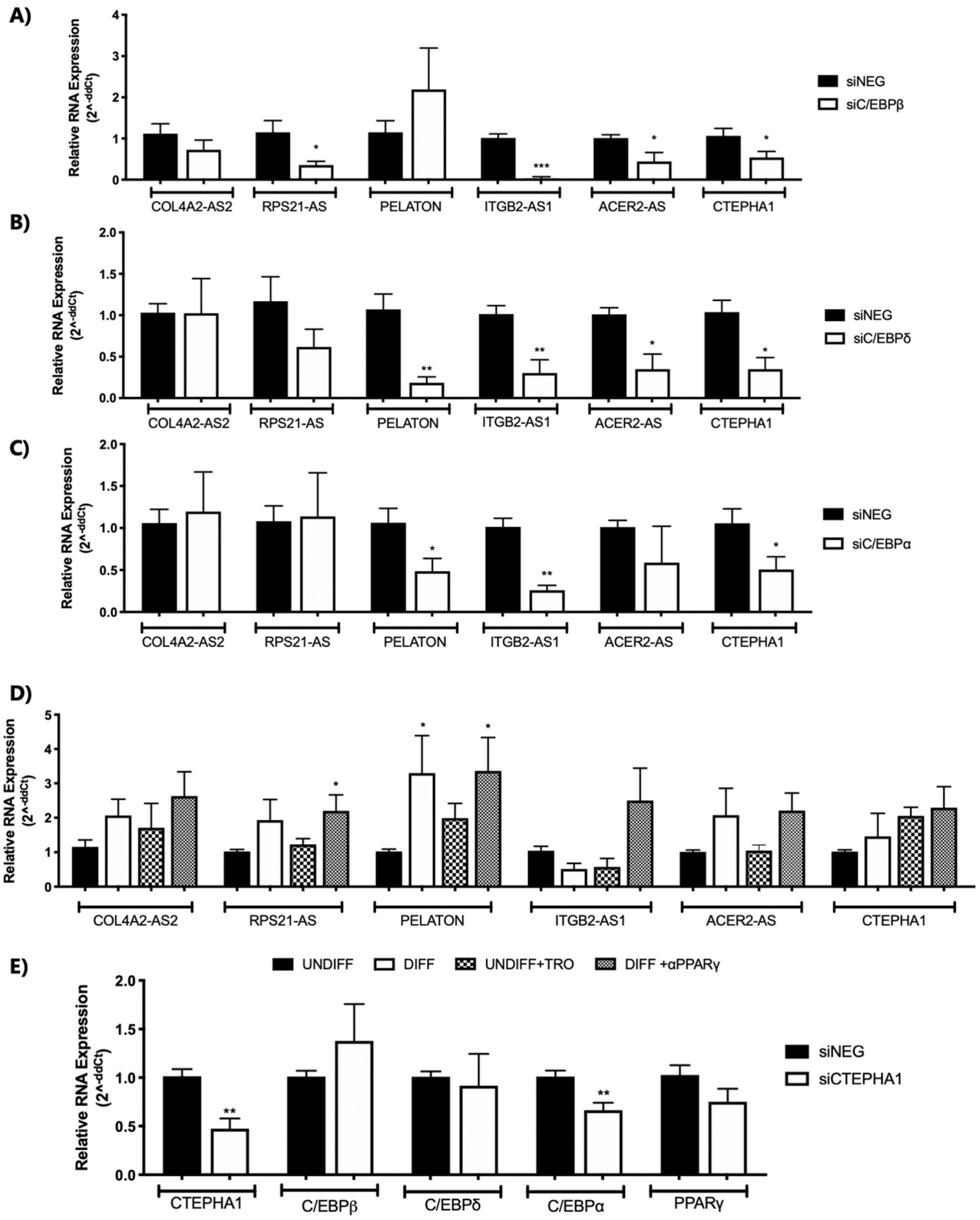

Fig. 6. Adipogenic transcription factors modulation of lncRNAs and sense genes. Differential expression of lncRNAs in hADSCs silenced for C/EBPβ (A), C/EBPδ (B), C/EBPα (C) versus control (siNEG) was verified by Real Time PCR. 18S was used as housekeeping gene. Data are expressed as mean of 3 experiments each performed in duplicates ± SEM (n = 6), * $p < 0.05$, ** $p < 0.01$, *** $p < 0.001$ vs siNEG. (D) Expression of lncRNAs in hADSCs from healthy patients treated in undifferentiated conditions (UNDIFF), differentiated for 7 days in standard adipogenic medium (DIFF), in undifferentiated condition supplemented with Troglitazone (UNDIFF+TRO) and differentiated for 7 days in standard adipogenic medium supplemented with the PPARγ inhibitor T0070907 (DIFF + αPPARγ). Expression was verified by Real Time PCR and 18S was used as housekeeping gene. Data are expressed as mean of 3 experiments each performed in duplicates ± SEM (n = 6), * $p < 0.05$, vs UNDIFF. (E) Expression of CTEPHA1 and adipogenic genes in hADSCs silenced for CTEPHA1. 18S was used as housekeeping gene. Data are expressed as mean of 3 experiments each performed in duplicates ± SEM (n = 6), ** $p < 0.01$ vs siNEG.

3.6. The lncRNA CTEPHA1 could have a role in adipogenesis through the modulation of C/EBPα expression

To further understand the complex network of involvement for lncRNAs in adipogenesis we decided to modulate the expression of CTEPHA1 via RNA interference and subsequently assess the expression levels of adipogenesis-related genes (C/EBPβ, C/EBPδ, C/EBPα and PPARγ). We found a successful inhibition of CTEPHA1, and we report that this does not appear to influence the early adipogenesis regulators C/EBPβ and C/EBPδ (Fig. 6E). On the contrary, its inhibition appears to be correlated with the reduced expression of C/EBPα and PPARγ, suggesting that CTEPHA1 could influence later stages of adipogenesis. Indeed, the most significant down-regulation is observed for C/EBPα, and this could be the TFs on which CTEPHA1 acts the most, in a positive feedback loop even as C/EBPα's downregulation also inhibits CTEPHA1 (Fig. 6C, Fig. 6E).

3.7. Role of the coding transcriptome in SAT from obese patients

We subsequently decided to perform a comprehensive in silico dissection of the deregulated dataset, and in order to ensure a higher significance for the in silico prediction, we selected those genes with an FDR ≤ 0.05. We thus obtained a total of 83 genes, of which 3 were non coding genes (Table 4, Table S8).

We then decided to analyze the top 20 DE RNAs based on their FC (Table 5). These include lncRNAs (COL4A2-AS2), along with genes implicated in the immune system, tissue re-modelling and biology of striatal muscle.

The subcellular localization of a protein can help infer its possible function, and moreover a global look at the localization of the DE RNAs can help identify the compartments most affected by the dysregulation. When looking at the subcellular localization of DE RNAs, a high number of organelles emerge, suggesting that the cells of the SAT present with ubiquitary perturbations, in the nucleus as well as the cytoplasm, the mitochondria, and the cytoskeleton indicating a profound alteration in all cellular functions (Fig. 7A).

3.8. GO terms enrichment and pathways analysis

We then performed a GSEA for GO and pathways analysis, in order to consider the whole perturbation happening in SAT (Fig. 7B–F). The Biological Processes analysis highlighted positive enrichment involved in immune system response (B cell activation and antigen receptor signaling pathway), whilst there is a negative enrichment for metabolic processes (ATP and amino acid) (Fig. 7B). Similarly, Molecular Function also highlighted a positive enrichment in immune system process and channel activity (Fig. 7C). Interestingly, a negative enrichment is present for gene expression modulation, with processes implicated in transcription and translation (Fig. 7C). Concordantly, Cellular Component analysis highlighted a positive enrichment in immune-related complexes whilst a negative enrichment in nuclear and mitochondrial components (Fig. 7D). KEGG pathway analysis highlighted also a positive enrichment in genes associated with autoimmune diseases (e.g. autoimmune thyroid disease, systemic lupus erythematosus and asthma), whilst there is a negative enrichment in metabolic pathways (Fig. 7E). WikiPathways analysis also shows the same results (Fig. 7F).

Table 4
Number of differentially expressed genes with FDR ≤ 0.05 in SAT of OBF vs. CTRL.

	OBF vs. CTRL		
	mRNAs	ncRNAs	Total
Up Regulated	57	2	59
Down Regulated	23	1	24
Total	80	3	83

Table 5
FC of Top 20 DE RNAs. Protein function description was obtained from the STRING database.

Gene Name	FC	p value	Protein Function
COL4A2-AS2	5.93	0.00014	//
MMP7	5.72	0.000018	Matrilysin; Degrades casein, gelatins of types I, III, IV, and V, and fibronectin.
DES	−5.67	0.00000026	Desmin; Muscle-specific type III intermediate filament essential for proper muscular structure and function.
ADAMDEC1	5.26	0.000018	Important role in the control of the immune response.
TREM2	5.20	0.0000011	Triggering receptor expressed on myeloid cells 2; Forms a receptor signaling complex with TYROBP.
SPP1	5.09	0.0000071	Osteopontin; Binds tightly to hydroxyapatite. Forms an integral part of the mineralized matrix. Important to cell-matrix interaction.
TM4SF19	4.98	0.0000034	Transmembrane 4 L six family member 19; Belongs to the L6 tetraspanin family.
MMP8	4.70	0.000028	Neutrophil collagenase; Can degrade fibrillar type I, II, and III collagens; Belongs to the peptidase M10A family.
DCSTAMP	4.63	0.000025	Dendritic cell-specific transmembrane protein; Cell surface receptor, roles in cellular fusion, cell differentiation, bone and immune homeostasis. Role in TNFSF11-mediated osteoclastogenesis.
ACP5	4.50	0.00664	Tartrate-resistant acid phosphatase type 5; Involved in osteopontin/bone sialoprotein dephosphorylation. Belongs to the metallophosphoesterase superfamily.
ANLN	4.44	0.0076	Anillin; Required for cytokinesis. Essential for the structural integrity of the cleavage furrow and for completion of cleavage furrow ingression. Plays a role in bleb assembly during metaphase and anaphase of mitosis.
PDE6G	4.32	0.000016	Retinal rod rhodopsin-sensitive cGMP 3′,5′-cyclic phosphodiesterase subunit gamma; Implicated in transmission of the visual signal.
ACTG2	−4.27	0.011	Actin, gamma-enteric smooth muscle; Actins are highly conserved proteins that are involved in various types of cell motility and are ubiquitously expressed in all eukaryotic cells.
TM4SF19-TCTEX1D2	4.12	0.00011	//
SDS	4.10	0.000015	L-serine dehydratase/L-threonine deaminase; Serine dehydratase.
TNNI2	3.96	0.00021	Troponin I, fast skeletal muscle; Inhibitory subunit of troponin, the thin filament regulatory complex which confers calcium-sensitivity to striated muscle actomyosin ATPase activity.
SDC1	3.94	0.029	Syndecan-1; Cell surface proteoglycan that bears both heparan sulfate and chondroitin sulfate and that links the cytoskeleton to the interstitial matrix. Regulates exosome biogenesis in concert with SDCBP and PDCD6IP
CD300LB	3.77	0.000038	CMRF35-like molecule 7; Acts as an activating immune receptor through its interaction with ITAM-bearing adapter TYROBP, and also independently by recruitment of GRB2.
APOC1	3.75	0.00000075	Apolipoprotein C-I; Inhibitor of lipoprotein binding to the low-density lipoprotein (LDL) receptor, LDL receptor-related protein, and very low-density lipoprotein (VLDL) receptor.
CD52	3.73	0.000013	CAMPATH-1 antigen; May play a role in carrying and orienting carbohydrate, as well as having a more specific role.

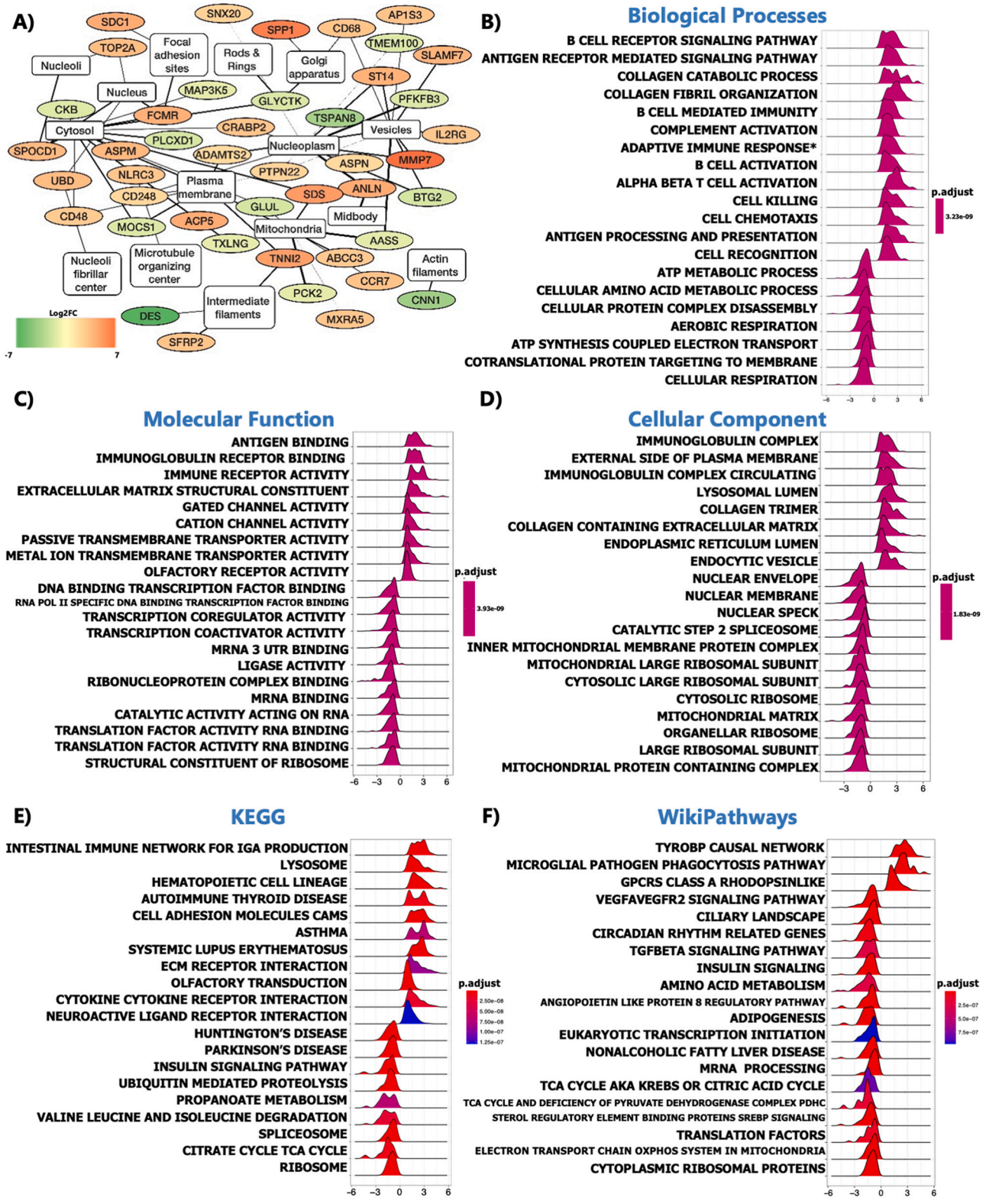

Fig. 7. Characterization of coding DE RNAs and enrichment analysis (A) Subcellular localization of deregulated genes as obtained with the NDEx database. Gene set enrichment analysis was performed on clusterProfiler R package. Gene set from Molecular Signature databases such as curated gene set (C2) and ontology gene sets (C5) and a p value cut off <0.05 were considered for this analysis. The top 20 BP (B), MF (C), CC (D), KEGG (E) and WikiPathways (F) enriched pathways obtained with GSEA are reported as ridge plot, where the x axis refers to the enrichment score and the color scale to the p-value. Adaptative immune response* in (B) refers to "adaptive immune response based on somatic recombination of immune receptors built from immunoglobulin superfamily domains".

3.9. Obesity association with co-occurring diseases

As obesity is known to increase the risk of co-morbidities development, we aimed to identify which deregulated genes are specifically responsible for this phenomenon. Via the DisGENET database we reported the known interaction of the DE RNAs with an FDR ≤ 0.05 with diseases of Nutritional and Metabolic Diseases and the Immune System, obtained from curated databases (Fig. 8A, B). When we analyzed all

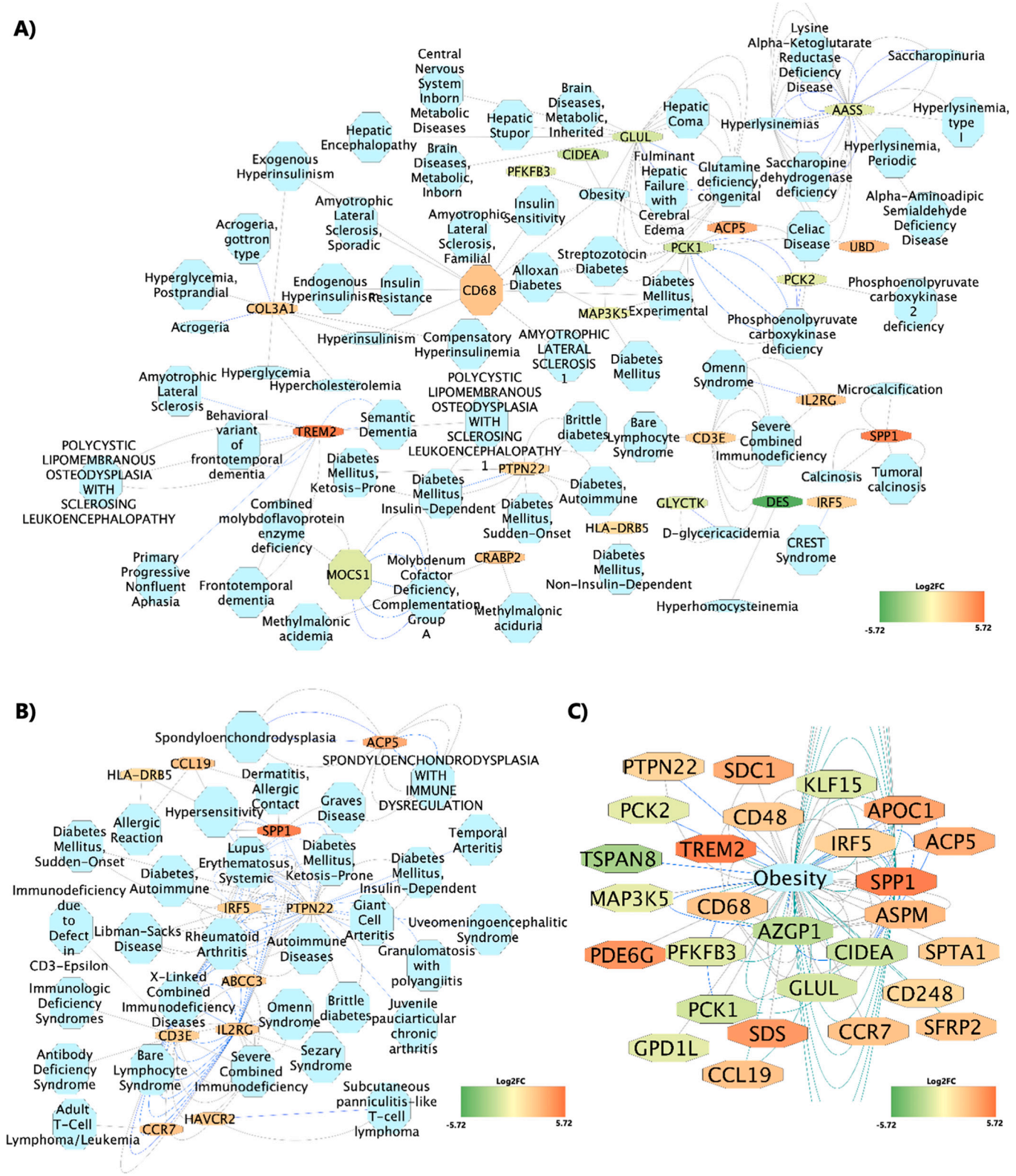

Fig. 8. Transcriptional characterization identifies gene signature associated with disease occurrence. DisGENET analysis shows the DE RNAs terms with an FDR $\leq$ 0.05 implicated in (A), nutritional and metabolic diseases (B) immune system and (C) in obesity in SAT from OBF vs CTRL. The lines connecting the genes to the disease term represent the literature evidence for the terms' implication in the disease. The color scale represents the genes FC.

known interactions between the DE RNAs and nutritional and metabolic diseases as obtained from curated databases we found canonical metabolic diseases such as diabetes and celiac disease, along with diseases of the central nervous system diseases with a metabolic component, such as central nervous system inborn metabolic diseases, brain metabolic diseases, amyotrophic lateral sclerosis, semantic dementia etc. (Fig. 8A). For the Immune System, numerous diseases were implicated including multiple types of diabetes, known complication of obesity, but also autoimmune diseases such as Lupus Erythematosus Systemic, Rheumatoid Arthritis, Immunologic Deficiency Syndromes, Multiple Sclerosis, defects in the leucocyte adhesion process, dermal diseases etc. (Fig. 8B). When expanding the search to all known databases, 27 genes were found to be significantly associated with obesity (Fig. 8C). As negative controls, we run the gene-set against un-related disease classes such as "infections" and "animal diseases", which returned no terms. Moreover, we run a search of 83 randomly selected terms (Table S9) for the same databases, and the correlations present are reported for nutritional and metabolic diseases (Fig. S9A), immune system diseases (Fig. S9B) and obesity in all known databases (Fig. S9C). In these cases, only two genes per network emerged, highlighting that the connection reported in Fig. 8 is specific of our dataset.

4. Discussion

Obesity is a very severe condition which can lead to an increase in associated morbidities for many chronic diseases such as T2D, hypertension, coronary artery disease, dyslipidemia, stroke, osteoarthritis, certain forms of cancer [1–3], and ultimately result in an increased mortality rate [1]. To this day, it is not possible to have conclusive data on what is the relative contribution of either genetic or the environment on obesity onset. Indeed, behavior and genes are different levels of the same causal framework, and epigenetics through RNA biology has been suggested to play a central role in elucidating new targetable pathways. We previously highlighted the presence of different transcriptional profiles in obesity-affected men and women, highlighting gender-specific differences in transcription profiles, and we also performed a characterization of the oncogenic susceptibility present in SAT tissues of normal weight subjects, obesity-affected women, obesity and type 2 diabetes-affected women and obesity-affected men [4,22]. In this study we have characterized the differences in the transcriptional profiles of SAT from normal weight and obesity-affected women, with a particular interest on the role of long non-coding RNAs. Remarkably, amongst the 171 DE RNAs identified here, 81 had never been correlated to obesity before and could thus be of great relevance for future characterization in the obesogenic context. The non-coding transcriptome was found to be significantly implicated, and we focused our further characterization on lncRNAs as this class of molecules are showing to have a relevant function in the pathogenesis of numerous metabolic diseases, including obesity [16,42–45]. The identification of co-interaction networks allowed us to identify 6 lncRNAs which could influence numerous coding genes found altered via RNA-seq, thus suggesting a potential their involvement in the altered signaling pathways present in obesity [22,46,47]. The 6 lncRNAs identified were COL4A2-AS2, RPS21-AS, PELATON, ITGB2-AS1, ACER2-AS and CTEPHA1, and for each of them we performed a further characterization both in silico and in vitro during the differentiation of hADSCs. We report that these are expressed in the adipose tissue, present binding sites for adipogenesis-related TFs and are also implicated in adipogenesis related biological processes such as regulation of fat cell differentiation (COL4A2-AS2), immune response (PELATON, ITGB2-AS1 and CTEPHA1) and metabolic processes (ACER2-AS).

When analyzing their deregulation in different phases of adipogenic differentiation process, they all present different expression levels during adipogenesis in mesenchymal stem cells obtained from both obese and healthy subjects. Although these are different biological scenarios compared to the whole tissue analysis, performed through RNA-seq, these in vitro models allow to question whether the dysfunctions observed in SAT could be recapitulated in early stages of tissue development, such as those represented by adipogenesis. Interestingly, whilst the RNA-seq characterized coding and non-coding genes implicated in obese-derived SAT, we found an implication for the investigated lncRNAs also in adipogenesis processes of healthy patients, suggesting a role for these molecules in the regulation of the process.

We identified, for the first time, a modulation of the lncRNAs by C/EBPβ, C/EBPδ and C/EBPα, along with a role for PPARγ in modulating these genes. Even if the genes do not present binding sites for all these transcription factors, there could be a trans modulation of the lncRNAs expression, as these are primary regulators of a network that is indeed complex and rich in other key players [48,49]. Specifically, the lncRNAs expression appears to be impacted mostly by C/EBPs dysregulation in expression. Moreover, we investigated whether the lncRNAs, focusing on CTEPHA1, could also influence the TFs expression, and found that CTEPHA1 inhibition also led to a decreased expression in late adipogenesis modulators, with a specific relevance for C/EBPα. Indeed, adipogenesis is a complex network governed by a multitude of regulators, and lncRNAs could be important players in it [48–50]. These molecules present modes of action both in cis, in proximity to their gene locus, and in trans, governing the action of genes which do not necessarily relate to their chromosomal localization [15,16,21,45,51].

We also performed a dissection of localization and pathways dysregulation from coding genes, and found a significant implication for the immune system, to be expected as the SAT from obese patients presents a high degree of flogosis, along with tissue remodeling and, interestingly, the biology of the striatal muscle. Indeed, obesity can cause a decline in contractile function of skeletal muscle, thereby reducing mobility and leading to the development of even more obesity-associated health risks [52]. KEGG and WikiPathways analyses highlighted also a positive enrichment in genes associated with autoimmune diseases (e.g. autoimmune thyroid disease, systemic lupus erythematosus and asthma), whilst there is a negative enrichment in metabolic pathways. The gene expression signature is also correlated with multiple diseases insurgence, such as immune system diseases and nutritional and metabolic system diseases. The research presented here was possibly limited by the small sample-size and further technical validation in different adipose depots as well as confirmation data in wider cohorts with related follow-up studies are certainly needed.

Overall, our findings are a thorough characterization of transcriptional dysregulation present in subcutaneous adipose tissue of obesity-affected patients. Our results highlight a clear implication for 6 never described lncRNAs in adipogenesis network, adding them as new players and regulators to the adipocyte biology, with implications for human obesity. Indeed, these molecules could prove to be biomarkers relevant for early intervention, or useful tools in the development of future precision medicine strategies.

Supplementary data to this article can be found online at https://doi.org/10.1016/j.ygeno.2021.09.014.

Declaration of competing interest

The authors declare that they have no conflict of interest.

Acknowledgments

FR would like to acknowledge and thank the Fondazione Fratelli Confalonieri for financial support during her PhD. This work was supported by a grant from the Pediatric Clinical Research Center Fondazione "Romeo and Enrica Invernizzi" to GVZ and SC.

References

[1] WHO, Obesity and Overweight World Health Organization [Available from: https://www.who.int/news-room/fact-sheets/detail/obesity-and-overweight, 2020.

[2] D. Haslam, N. Sattar, M. Lean, ABC of obesity. Obesity—time to wake up, BMJ 333 (7569) (2006) 640–642.
[3] V.J. Lawrence, P.G. Kopelman, Medical consequences of obesity, Clin. Dermatol. 22 (4) (2004) 296–302.
[4] F. Rey, L. Messa, C. Pandini, R. Launi, B. Barzaghini, G. Micheletto, et al., Transcriptome analysis of subcutaneous adipose tissue from severely obese patients highlights deregulation profiles in coding and non-coding oncogenes, Int. J. Mol. Sci. 22 (4) (2021).
[5] H.R. Wyatt, Update on treatment strategies for obesity, J. Clin. Endocrinol. Metab. 98 (4) (2013) 1299–1306.
[6] R.K. Singh, P. Kumar, K. Mahalingam, Molecular genetics of human obesity: a comprehensive review, C R Biol. 340 (2) (2017) 87–108.
[7] R. Stöger, Epigenetics and obesity, Pharmacogenomics 9 (12) (2008) 1851–1860.
[8] M. Loh, L. Zhou, H.K. Ng, J.C. Chambers, Epigenetic disturbances in obesity and diabetes: epidemiological and functional insights, Mol. Metabol. 27 (2019) S33–S41.
[9] F. Allum, E. Grundberg, Capturing functional epigenomes for insight into metabolic diseases, Mol. Metabol. 38 (2020) 100936.
[10] G. St Laurent, C. Wahlestedt, P. Kapranov, The landscape of long noncoding RNA classification, Trends Genet. 31 (5) (2015) 239–251.
[11] G. Boden, X. Duan, C. Homko, E.J. Molina, W. Song, O. Perez, et al., Increase in endoplasmic reticulum stress-related proteins and genes in adipose tissue of obese, insulin-resistant individuals, Diabetes. 57 (9) (2008) 2438–2444.
[12] P. Arner, A. Kulyté, MicroRNA regulatory networks in human adipose tissue and obesity, Nat. Rev. Endocrinol. 11 (5) (2015) 276–288.
[13] J. Chen, X. Cui, C. Shi, L. Chen, L. Yang, L. Pang, et al., Differential lncRNA expression profiles in brown and white adipose tissues, Mol. Gen. Genomics. 290 (2) (2015) 699–707.
[14] L. Sun, L.A. Goff, C. Trapnell, R. Alexander, K.A. Lo, E. Hacisuleyman, et al., Long noncoding RNAs regulate adipogenesis, Proc. Natl. Acad. Sci. U. S. A. 110 (9) (2013) 3387–3392.
[15] H. Gao, A. Kerr, H. Jiao, C.C. Hon, M. Rydén, I. Dahlman, et al., Long non-coding RNAs associated with metabolic traits in human white adipose tissue, EBioMedicine 30 (2018) 248–260.
[16] F. Rey, V. Urrata, L. Gilardini, S. Bertoli, V. Calcaterra, G.V. Zuccotti, et al., Role of long non-coding RNAs in adipogenesis: state of the art and implications in obesity and obesity-associated diseases, Obes. Rev. 22 (7) (2021) 1–19.
[17] J.R. Alvarez-Dominguez, Z. Bai, D. Xu, B. Yuan, K.A. Lo, M.J. Yoon, et al., De novo reconstruction of adipose tissue transcriptomes reveals long non-coding RNA regulators of brown adipocyte development, Cell Metab. 21 (5) (2015) 764–776.
[18] E.S.B. Salem, A.D. Vonberg, V.J. Borra, R.K. Gill, T. Nakamura, RNAs and RNA-binding proteins in immuno-metabolic homeostasis and diseases, Front. Cardiovasc. Med. 6 (2019) 106.
[19] J.F. Landrier, A. Derghal, L. Mounien, MicroRNAs in obesity and related metabolic disorders, Cells 8 (8) (2019).
[20] C. Arcinas, W. Tan, W. Fang, T.P. Desai, D.C.S. Teh, U. Degirmenci, et al., Adipose circular RNAs exhibit dynamic regulation in obesity and functional role in adipogenesis, Nat. Metabol. 1 (7) (2019) 688–703.
[21] F. Rey, G.V. Zuccotti, S. Carelli, Long non-coding RNAs in metabolic diseases: from bench to bedside, Trends Endocrinol. Metab. 32 (10) (2021) 747–749.
[22] F. Rey, L. Messa, C. Pandini, E. Maghraby, B. Barzaghini, M. Garofalo, et al., RNA-seq characterization of sex-differences in adipose tissue of obesity affected patients: computational analysis of differentially expressed coding and non-coding RNAs, J. Pers. Med. 11 (5) (2021).
[23] C.C. Gerhardt, I.A. Romero, R. Cancello, L. Camoin, A.D. Strosberg, Chemokines control fat accumulation and leptin secretion by cultured human adipocytes, Mol. Cell. Endocrinol. 175 (1–2) (2001) 81–92.
[24] G. Yu, L.G. Wang, Y. Han, Q.Y. He, clusterProfiler: an R package for comparing biological themes among gene clusters, OMICS 16 (5) (2012) 284–287.
[25] A. Zhu, J.G. Ibrahim, M.I. Love, Heavy-tailed prior distributions for sequence count data: removing the noise and preserving large differences, Bioinformatics 35 (12) (2019) 2084–2092.
[26] D. Pratt, J. Chen, D. Welker, R. Rivas, R. Pillich, V. Rynkov, et al., NDEx, the network data exchange, Cell Syst. 1 (4) (2015) 302–305.
[27] P. Shannon, A. Markiel, O. Ozier, N.S. Baliga, J.T. Wang, D. Ramage, et al., Cytoscape: a software environment for integrated models of biomolecular interaction networks, Genome Res. 13 (11) (2003) 2498–2504.
[28] J. Li, D. Zhou, W. Qiu, Y. Shi, J.-J. Yang, S. Chen, et al., Application of weighted gene co-expression network analysis for data from paired design, Sci. Rep. 8 (1) (2018) 622.
[29] L. Ke, D.C. Yang, Y. Wang, Y. Ding, G. Gao, AnnoLnc2: the one-stop portal to systematically annotate novel lncRNAs for human and mouse, Nucleic Acids Res. 48 (W1) (2020). W230-W8.
[30] Z. Li, L. Liu, S. Jiang, Q. Li, C. Feng, Q. Du, et al., LncExpDB: an expression database of human long non-coding RNAs, Nucleic Acids Res. 49 (D1) (2021). D962-D8.
[31] S. Carelli, F. Messaggio, A. Canazza, D.M. Hebda, F. Caremoli, E. Latorre, et al., Characteristics and properties of mesenchymal stem cells derived from microfragmented adipose tissue, Cell Transplant. 24 (7) (2015) 1233–1252.
[32] S. Carelli, M. Colli, V. Vinci, F. Caviggioli, M. Klinger, A. Gorio, Mechanical activation of adipose tissue and derived mesenchymal stem cells: novel anti-inflammatory properties, Int. J. Mol. Sci. 19 (1) (2018).
[33] A. Kawaji, Y. Ohnaka, S. Osada, M. Nishizuka, M. Imagawa, Gelsolin, an actin regulatory protein, is required for differentiation of mouse 3T3-L1 cells into adipocytes, Biol. Pharm. Bull. 33 (5) (2010) 773–779.
[34] F. Rey, E. Lesma, D. Massihnia, E. Ciusani, S. Nava, C. Vasco, et al., Adipose-derived stem cells from fat tissue of breast cancer microenvironment present altered adipogenic differentiation capabilities, Stem Cells Int. 2019 (2019) 1480314.
[35] B. Galateanu, S. Dinescu, A. Cimpean, A. Dinischiotu, M. Costache, Modulation of adipogenic conditions for prospective use of hADSCs in adipose tissue engineering, Int. J. Mol. Sci. 13 (12) (2012) 15881–15900.
[36] G.J. Hausman, M.V. Dodson, K. Ajuwon, M. Azain, K.M. Barnes, L.L. Guan, et al., Board-invited review: the biology and regulation of preadipocytes and adipocytes in meat animals, J. Anim. Sci. 87 (4) (2009) 1218–1246.
[37] G. Lee, F. Elwood, J. McNally, J. Weiszmann, M. Lindstrom, K. Amaral, et al., T0070907, a selective ligand for peroxisome proliferator-activated receptor gamma, functions as an antagonist of biochemical and cellular activities, J. Biol. Chem. 277 (22) (2002) 19649–19657.
[38] K.J. Livak, T.D. Schmittgen, Analysis of relative gene expression data using real-time quantitative PCR and the 2(-Delta Delta C(T)) Method, Methods 25 (4) (2001) 402–408.
[39] M. Zhou, X. Guo, M. Wang, R. Qin, The patterns of antisense long non-coding RNAs regulating corresponding sense genes in human cancers, J. Cancer 12 (5) (2021) 1499–1506.
[40] H. Zhuang, X. Zhang, C. Zhu, X. Tang, F. Yu, G.W. Shang, et al., Molecular mechanisms of PPAR-γ governing MSC osteogenic and adipogenic differentiation, Curr. Stem Cell Res. Ther. 11 (3) (2016) 255–264.
[41] M.I. Lefterova, A.K. Haakonsson, M.A. Lazar, S. Mandrup, PPARγ and the global map of adipogenesis and beyond, Trends Endocrinol. Metab. 25 (6) (2014) 293–302.
[42] T. Squillaro, G. Peluso, U. Galderisi, G. Di Bernardo, Long non-coding RNAs in regulation of adipogenesis and adipose tissue function, Elife 9 (2020).
[43] S.N. Wijesinghe, T. Nicholson, K. Tsintzas, S.W. Jones, Involvements of long noncoding RNAs in obesity-associated inflammatory diseases, Obes. Rev. 22 (4) (2020) 1–14.
[44] S. Babapoor-Farrokhran, D. Gill, R.T. Rasekhi, The role of long noncoding RNAs in atrial fibrillation, Heart Rhythm. 17 (6) (2020) 1043–1049.
[45] E. Ji, C. Kim, W. Kim, E.K. Lee, Role of long non-coding RNAs in metabolic control, Biochim. Biophys. Acta Gene Regul. Mech. 1863 (4) (2020) 194348.
[46] S. Tait, A. Baldassarre, A. Masotti, E. Calura, P. Martini, R. Varì, et al., Integrated transcriptome analysis of human visceral adipocytes unravels dysregulated microRNA-long non-coding RNA-mRNA networks in obesity and colorectal cancer, Front. Oncol. 10 (2020) 1089.
[47] Y. Chen, K. Li, X. Zhang, J. Chen, M. Li, L. Liu, The novel long noncoding RNA lncRNA-Adi regulates adipogenesis, Stem Cells Transl. Med. 9 (9) (2020) 1053–1067.
[48] J.E. Lee, H. Schmidt, B. Lai, K. Ge, Transcriptional and epigenomic regulation of adipogenesis, Mol. Cell. Biol. 39 (11) (2019).
[49] W. Kuri-Harcuch, C. Velez-delValle, A. Vazquez-Sandoval, C. Hernández-Mosqueira, V. Fernandez-Sanchez, A cellular perspective of adipogenesis transcriptional regulation, J. Cell. Physiol. 234 (2) (2019) 1111–1129.
[50] A.L. Ghaben, P.E. Scherer, Adipogenesis and metabolic health, Nat. Rev. Mol. Cell Biol. 20 (4) (2019) 242–258.
[51] J. Latorre, J.M. Fernández-Real, LncRNAs in adipose tissue from obese and insulin-resistant subjects: new targets for therapy? EBioMedicine 30 (2018) 10–11.
[52] J. Tallis, R.S. James, F. Seebacher, The effects of obesity on skeletal muscle contractile function, J. Exp. Biol. 221 (Pt 13) (2018).